Available online at www.sciencedirect.com
SCIENCE DIRECT®
Journal of Sound and Vibration 285 (2005) 941–966
JOURNAL OF SOUND AND VIBRATION
www.elsevier.com/locate/jsvi

Free in-plane vibration analysis of rectangular plates with elastic support normal to the boundaries

D.J. Gorman*

Department of Mechanical Engineering, The University of Ottawa, 770 King Edward Avenue, Ottawa, Canada K1N 6N5

Received 23 January 2004; received in revised form 8 September 2004; accepted 10 September 2004
Available online 26 January 2005

Abstract

The superposition method is employed to analyze the effects of elastic edge support on the in-plane free vibration frequencies and mode shapes of rectangular plates. The elastic edge support is considered to be uniformly distributed along the plate edges and symmetrically distributed with respect to the plate central axes. In addition, exact solutions are also obtained for a family of simply supported plates whose eigenvalues constitute upper limits for those of the elastically supported plates. An array of highly accurate eigenvalues for the completely free plate is also computed in order to provide lower limit eigenvalues. Eigenvalues are computed and tabulated for elastically supported plates of various aspect ratios and dimensionless elastic support coefficients.

1. Introduction

It is generally agreed that there exists a vast technical literature related to the free lateral vibration of rectangular plates. The situation with regard to in-plane vibration is quite different. There are, nevertheless, a limited number of publications related to this latter subject, most of which have appeared in recent years. Since listings of these publications have appeared in Refs. [1–3], for example, there is no need to repeat them here.

*Tel.: +1 613 562 5800; fax: +1 613 562 5177.
E-mail address: dgorman@genie.uottawa.ca (D.J. Gorman).

0022-460X/$ - see front matter © 2004 Elsevier Ltd. All rights reserved.
doi:10.1016/j.jsv.2004.09.017

Nomenclature

a, b	quarter plate edge lengths
a_{11}	$= 1$
a_{12}	$= -v$
a_{66}	$= (1 - v)/2$
E	Young's modulus of plate material
k_1, k_2	basic elastic edge stiffnesses, defined in text
K_1^*, K_2^*	dimensionless elastic edge stiffnesses, defined in text
u, v	plate in-plane displacements in x and y directions, respectively
U, V	dimensionless displacements, $U = u/a$, $V = v/a$
x, y	quarter plate coordinates
ξ, η	dimensionless coordinates, $\xi = x/a$, $\eta = y/b$
φ	plate aspect ratio, b/a
$\varphi^{\|}$	inverse of plate aspect ratio, a/b
$\sigma_x^*, \sigma_y^*, \tau_{xy}^*$	dimensionless in-plane normal and shear stresses, defined in text
ω	circular frequency of plate vibration
ρ	mass density of plate material
v	Poisson ratio of plate material (taken here as 0.3)
λ^2	dimensionless frequency of plate vibration, $= \omega a\sqrt{\rho(1 - v^2)/E}$

It is acknowledged that lateral vibration problems have historically received most of the attention as their lower natural vibration frequencies are more likely to coincide with those of the available excitation forces. It is pointed out, however, that there is a legitimate practical need for exploration of plate in-plane vibration. Such vibration can be encountered when turbulent fluid boundary layers flow along plate structures such as ship hulls. Another practical application where in-plane plate vibration can be encountered centers around the dynamic behavior of sandwich plates. Here the outer sheets of the assembly may undergo in-plane vibration, while the assembly itself undergoes lateral vibration. This phenomenon is discussed by Wang and Wereley [4].

In an earlier publication, the present author described how highly accurate analytical type solutions are obtained for in-plane free vibration of the completely free rectangular plate [2]. Subsequently, he described the obtaining of solutions for the fully clamped plate [3]. In both studies the analysis was carried out by means of the superposition method. In the latter paper, it was also shown how exact Levy type solutions can be obtained for a family of simply supported plates. In both cases excellent agreement was encountered when computed results were compared with those obtained by Bardel et al. [1] using a Rayleigh–Ritz energy approach.

In the present paper, the superposition method is employed to obtain accurate analytical type solutions for the free in-plane vibration of rectangular plates with uniform, symmetrically distributed elastic edge supports acting normal to the boundaries. All plate boundaries are free of shear stresses. Stresses normal to these boundaries are, of course, proportional to plate displacement normal to these same boundaries. The magnitude of these stresses will depend on the elastic stiffness of the edge support. Exact Levy type solutions are also obtained for an additional set of problems where the boundary conditions are designated as those of the simple support type. These latter exact solutions provide limiting cases for the problems of plates with elastic support, as the stiffness of the support approaches infinity.

2. Mathematical procedure

2.1. The families of modes under investigation

The outline of a rectangular plate of interest is provided in Fig. 1. The reference, x, y, axes lie along the plate center lines. In all problems considered here the stiffness of the uniform elastic support running along opposite edges is considered to be equal. It is therefore to be anticipated that in-plane displacement patterns for all free vibration modes will possess symmetry, or anti-symmetry, with respect to the plate central axes. This phenomenon is discussed at length in Ref. [2]. A mode is said to possess symmetry with respect to an axis if plate displacement normal to the axis has a symmetric distribution about it. In such a case displacement parallel to the axis will have a displacement anti-symmetrically distributed about it. Modes with just the opposite displacement distributions are said to be anti-symmetrically distributed with respect to the axis. It is convenient, therefore, to define the three possible families of vibration modes as follows. (1) *Symmetric–symmetric modes*: these mode displacements have a symmetric distribution about each of the plate central axes. (2) *Anti-symmetric–anti-symmetric modes*: these mode displacements have an anti-symmetric distribution about each of the plate central axes. (3) *Symmetric–anti-symmetric modes*: these mode displacements possess symmetry with respect to the central x-axis, and anti-symmetry with respect to the central y-axis.

These three families represent all possible mode families for the plate under investigation and will be analyzed separately. It will be appreciated that with enforcement of appropriate boundary conditions only one-quarter of the plate need be analyzed.

It will also be appreciated that for each mode family there will be a limiting case approached when the elastic support stiffness coefficients approach infinity. In such limiting cases displacement normal to the boundaries will be forbidden as well as shear forces along the edges. It will be shown that exact solutions exist for the limiting cases of each of the three mode families

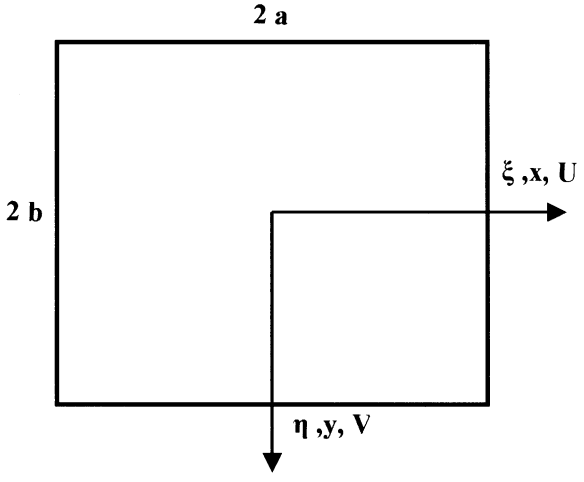

Fig. 1. Schematic representation of rectangular plate of interest.

discussed above. Because one-term exact solutions are obtained for these limiting cases, they are referred to here as simple support problems.

2.2. The governing differential equations

Equations governing the in-plane dynamic behavior of isotropic rectangular plates were developed in dimensionless form in Ref. [2]. They are reproduced here in the interest of completeness only:

$$a_{11}\frac{\partial^2 U}{\partial \xi^2}+\frac{a_{12}}{\phi}\frac{\partial^2 V}{\partial \xi \partial \eta}+\frac{a_{66}}{\phi}\left[\frac{\partial^2 V}{\partial \xi \partial \eta}+\frac{1}{\phi}\frac{\partial^2 U}{\partial \eta^2}\right]+\lambda^4 U=0 \tag{1}$$

and

$$a_{66}\left[\frac{\partial^2 V}{\partial \xi^2}+\frac{1}{\phi}\frac{\partial^2 U}{\partial \xi \partial \eta}\right]+\frac{a_{12}}{\phi}\frac{\partial^2 U}{\partial \eta \partial \xi}+\frac{a_{12}}{\phi^2}\frac{\partial^2 V}{\partial \eta^2}+\lambda^4 V=0, \tag{2}$$

where all symbols introduced are as defined in the nomenclature.

2.3. Dimensionless in-plane stresses and elastic support coefficients

The dimensionless in-plane stresses were developed in Ref. [2]. They are reproduced here for convenience as

$$\sigma_x^*=\frac{\partial U}{\partial \xi}+\frac{v}{\phi}\frac{\partial V}{\partial \eta},\quad \sigma_y^*=v\frac{\partial U}{\partial \xi}+\frac{1}{\phi}\frac{\partial V}{\partial \eta}\quad \text{and}\quad \tau_{xy}^*=\frac{\partial U}{\partial \eta}+\phi\frac{\partial V}{\partial \xi}.$$

Turning next to the elastic edge support coefficient, we first focus on the edge, $\eta=1$, of the quarter plate segment of Fig. 1. Returning to dimensional quantities and equating the plate in-plane normal tensile force per unit edge length to the matching force exerted by the elastic boundary, we obtain

$$\frac{E}{(1-v^2)}\left[v\frac{\partial u(x,y)}{\partial x}+\frac{\partial v(x,y)}{\partial y}\right]=-k_1 v(x,y), \tag{3}$$

where k_1 relates the force per unit depth of plate, per unit length, with plate displacement normal to the edge.

Non-dimensionalizing Eq. (3), it is readily shown that we may write

$$\sigma_y^*(\xi,\eta)=-K_1^* V(\xi,\eta), \tag{4}$$

where $K_1^*=k_1 a(1-v^2)/E$.

Following an identical procedure, it is shown that for the edge, $\xi=1$, we may write

$$\sigma_x^*(\xi,\eta)=-K_2^* U(\xi,\eta), \tag{5}$$

where $K_2^*=k_2 a(1-v^2)/E$, the subscript 2 referring to the edge, $\xi=1$. It is to be noted that for equal values of the basic stiffness coefficients, k_1 and k_2, the associated dimensionless coefficients K_1^* and K_2^* will be equal, regardless of the plate aspect ratio.

2.4. Analysis of symmetric–symmetric modes

The analytical procedure to follow differs very little from that described in detail in Ref. [2] for completely free plate analysis. Only these slight differences will be elaborated upon here.

Consider the quarter plate shown on the left-hand side of Fig. 2. Pairs of small circles adjacent to the axes indicate that free vibration modes will possess symmetry with respect to these axes. To the right of the figure the two forced vibration problems (building blocks) utilized in analyzing this family of modes by the superposition method are represented schematically. Distributed harmonic driving forces are represented by small arrows along the driven edges. Focusing on the first building block, it is seen that its response to the excitation may be expressed in the form proposed by Levy as

$$U(\xi,\eta)=\sum_{m=1,2}^{\infty} U_m(\eta)\cos \operatorname{emp}\xi \tag{6}$$

and

$$V(\xi,\eta)=\sum_{m=1,2}^{\infty} V_m(\eta)\sin \operatorname{emp}\xi, \tag{7}$$

where $\operatorname{emp}=(2m-1)\pi/2$.

The symmetric mode conditions are satisfied along the η-axis, while a condition of zero shear stress is satisfied along the edge, $\xi=1$. Stresses normal to this edge will in general be non-zero.

It is shown in detail in Ref. [2] how substitution of the above series into the differential equations leads to a pair of coupled ordinary differential equations involving the functions $U_m(\eta)$ and $V_m(\eta)$. Through differentiation and manipulation of these equations, a fourth-order ordinary homogeneous differential equation involving $V_m(\eta)$ only is isolated. The solution for this latter equation is well known.

Solving the related characteristic equation and introducing the quantities Root1, and Root2, which depend on the roots of the characteristic equation [2], it is shown that three forms of solution are possible for this differential equation for the problems under consideration. With each solution for the quantity $V_m(\eta)$, a solution for the corresponding quantity $U_m(\eta)$ is obtained using results of the previously manipulated equations [2]. Only the results are presented here for

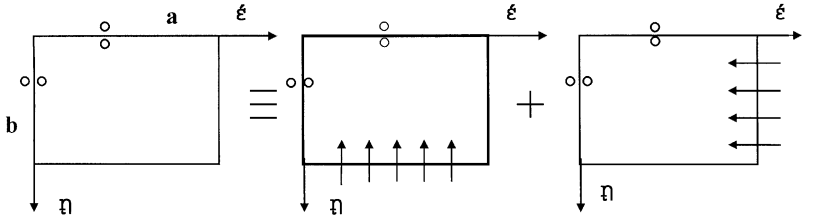

Fig. 2. Building blocks utilized in symmetric–symmetric mode analysis.

convenience. They are as follows.

Solution 1: Root1 $\geqslant 0$, Root2 $\leqslant 0$; then

$$V_m(\eta) = A_m \sinh \beta_m\eta + B_m \cosh \beta_m\eta + C_m \sin \gamma_m\eta + D_m \cos \gamma_m\eta \tag{8}$$

and

$$U_m(\eta) = A_m\alpha_{1m} \cosh \beta_m\eta + B_m\alpha_{2m} \sinh \beta_m\eta + C_m\alpha_{3m} \cos \gamma_m\eta + D_m\alpha_{4m} \sin \gamma_m\eta. \tag{9}$$

Solution 2: Root1 $\leqslant 0$, Root2 $\leqslant 0$; then

$$V_m(\eta) = A_m \sin \beta_m\eta + B_m \cos \beta_m\eta + C_m \sin \gamma_m\eta + D_m \cos \gamma_m\eta \tag{10}$$

and

$$U_m(\eta) = A_m\alpha_{1m} \cos \beta_m\eta + B_m\alpha_{2m} \sin \beta_m\eta + C_m\alpha_{3m} \cos \gamma_m\eta + D_m\alpha_{4m} \sin \gamma_m\eta. \tag{11}$$

Solution 3: Root1 $\geqslant 0$, Root2 $\geqslant 0$; then

$$V_m(\eta) = A_m \sinh \beta_m\eta + B_m \cosh \beta_m\eta + C_m \sinh \gamma_m\eta + D_m \cosh \gamma_m\eta \tag{12}$$

and

$$U_m(\eta) = A_m\alpha_{1m} \cosh \beta_m\eta + B_m\alpha_{2m} \sinh \beta_m\eta + C_m\alpha_{3m} \cosh \gamma_m\eta + D_m\alpha_{4m} \sinh \gamma_m\eta. \tag{13}$$

The quantities β_m, γ_m, $\alpha_{1m}, \ldots$ etc., are as defined in Ref. [2] and the quantities $A_m, B_m, \ldots$ etc., are to be determined through enforcement of appropriate boundary conditions.

It will be obvious, in view of the symmetry which the quantities, $V_m(\eta)$ above, must possess with respect to the ξ-axis, that the quantities A_m and B_m must all equal zero. Enforcement of the condition of zero shear force along the edge, $\eta = 1$, permits evaluation of a third coefficient. The quantities $V_m(\eta)$ and $U_m(\eta)$ for Solution 1 can therefore be expressed as

$$V_m(\eta) = B_m[\cosh \beta_m\eta + \theta_{1m} \cos \gamma_m\eta] \tag{14}$$

and

$$U_m(\eta) = B_m[\alpha_{2m} \sinh \beta_m\eta + \theta_{1m}\alpha_{4m} \sin \gamma_m\eta], \tag{15}$$

with corresponding expressions for the other solutions. Quantities θ_{1m} are given in Ref. [2].

It is here that the present analysis differs slightly from that of Ref. [2]. It is known that building blocks such as those under consideration may be either harmonically force-driven or displacement-driven. In some problems, however, it is found that use of displacement-driven building blocks is preferable. Use of force-driven building blocks can lead to the uncovering of what have been called 'rejection mode eigenvalues'. In this latter case, non-trivial solutions can be found for the coefficients in the distributed driving force expansions; however, displacement associated with one block nullifies exactly that associated with the other. The result is no net displacement for the plate in question and the associated eigenvalue must be rejected. This phenomenon as it pertains to plate lateral vibration has been discussed extensively in Ref. [5].

In the present analysis, we consider all building blocks to be displacement driven. Returning to Eq. (14) and continuing with analysis of the first building block, we choose to represent the amplitude of the displacement excitation along the driven edge as

$$V_m(\eta)|_{\eta=1} = \sum_{m=1,2}^{\infty} E_m \sin \operatorname{emp} \xi. \tag{16}$$

Enforcing this edge condition we obtain, for any m,

$$B_m[\cosh\ \beta_m + \theta_{1m}\cos\ \gamma_m] = E_m \tag{17}$$

and finally, Solution 1,

$$V_m(\eta) = E_m\theta_{11m}[\cosh\ \beta_m\eta + \theta_{1m}\cos\ \gamma_m\eta] \tag{18}$$

and

$$U_m(\eta) = E_m\theta_{11m}[\alpha_{2m}\sinh\ \beta_m\eta + \alpha_{4m}\sin\ \gamma_m\eta], \tag{19}$$

where $\theta_{11m} = 1/(\cosh\ \beta_m + \theta_{1m}\cos\ \gamma_m)$.

Corresponding expressions for Solutions 2 and 3 will differ in that, as seen earlier, they involve trigonometric functions and hyperbolic functions only, respectively, with expressions for the quantities θ_{11m} becoming $\theta_{11m} = 1/(\cos\ \beta_m + \theta_{1m}\cos\ \gamma_m)$ and $\theta_{11m} = 1/(\cosh\ \beta_m + \theta_{1m}\cosh\ \gamma_m)$, respectively.

It is to be noted that we now have available the solution for the response of the first building block to any harmonic edge displacement-driven excitation with the amplitude represented by the series of Eq. (16).

The second building block is displacement-driven along the edge, $\xi = 1$, and constitutes essentially a mirror image of the first. Its solution is easily extracted from that of the first following rules of transformation explained in Ref. [2], with the subscript 'm' now replaced by 'n' in order to avoid confusion. Retaining the symbols U and V to indicate displacements in the ξ and η directions, respectively, and interchanging the variables ξ and η in Eqs. (6) and (7), we obtain

$$U(\xi,\eta) = \sum_{n=1,2}^{\infty} U_n(\xi)\sin\ \mathrm{enp}\,\eta \tag{20}$$

and

$$V(\xi,\eta) = \sum_{n=1,2}^{\infty} V_n(\xi)\cos\ \mathrm{enp}\,\eta, \tag{21}$$

where $\mathrm{enp} = (2n-1)\pi/2$.

Before moving on to utilization of the above building block solutions for generation of the eigenvalue matrix associated with symmetric–symmetric mode analysis, it is appropriate to develop building block solutions for the other two families of modes.

2.5. Analysis of anti-symmetric–anti-symmetric modes

Again, the analysis will differ from that described for the corresponding set of modes in Ref. [2] only in that the building blocks will be displacement driven. The quarter plate of interest and associated building blocks utilized in the analysis are shown schematically in Fig. 3. Note that there are no pairs of small circles adjacent to the axes, indicating that this family of modes will have an anti-symmetric distribution with respect to the plate central axes. Focusing on the first

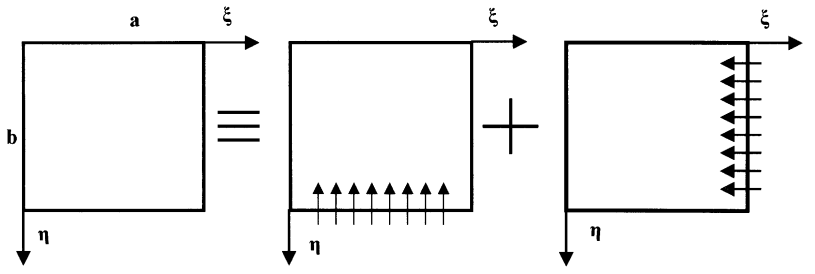

Fig. 3. Building blocks utilized in anti-symmetric–anti-symmetric mode analysis.

building block, its solution is expressed in the form proposed by Levy as

$$U(\xi,\eta)=\sum_{m=1,2}^{\infty}U_m(\eta)\sin \text{emp}\,\xi \tag{22}$$

and

$$V(\xi,\eta)=\sum_{m=1,2}^{\infty}V_m(\eta)\cos \text{emp}\,\xi, \tag{23}$$

where $\text{emp}=(m-1)\pi$.

As made clear in Ref. [2], the solution with $m=1$ will be one-dimensional with the quantity $U_m(\eta)$ equal to zero.

It is shown that upon satisfying the condition of anti-symmetry with respect to the ξ-axis the quantity $V_m(\eta)$ is expressed as

$$V_m(\eta)=A_0\ \sin\ \alpha\eta, \tag{24}$$

where $\alpha^2=\lambda^2\phi^2/a_{11}$, and A_0 is a constant to be determined. Quantity $a_{11}=$ unity.

The amplitude of the harmonically driven displacement along the edge, $\eta=1$, is expressed as

$$V_m(\eta)=\sum_{m=1,2}^{\infty}E_m\ \cos\ \text{emp}\,\xi. \tag{25}$$

Enforcing this edge condition for the first term of the expansion above ($m=1$), we obtain

$$A_0=E_m/\sin\alpha. \tag{26}$$

Returning to Eqs. (22) and (23), and considering the case $m\geqslant 1$, it is seen that solutions will be identical to those already provided in Ref. [2], except for the quantities θ_{11m}. Since we are now driving the building block with the distributed harmonic displacement of Eq. (25), new and appropriate expressions are required for these quantities as follows.

Solution 1:

$$\theta_{11m}=1/(\sinh\ \beta_m+\theta_{1m}\ \sin\ \gamma_m).$$

Solution 2:

$$\theta_{11m}=1/(\sin\ \beta_m+\theta_{1m}\ \sin\ \gamma_m).$$

Solution 3:

$$\theta_{11m} = 1/(\sinh \beta_m + \theta_{1m} \sinh \gamma_m).$$

This information, coupled with that of Ref. [2], provides the response of the first building block to any distributed harmonic edge excitation.

Response of the second building block is extracted from that of the first through the same transformation of axes as discussed earlier.

2.6. Analysis of the symmetric–anti-symmetric modes

This family of modes is analyzed by means of the building blocks of Fig. 4. The first building block differs from the one immediately above only in that it must possess symmetry with respect to the ξ-axis. For the term, $m = 1$, it is readily shown that we may write

$$V_m(\eta) = \frac{-E_m\phi}{\alpha \sin \alpha} \cos \alpha\eta. \tag{27}$$

Solutions for the response with $m \geqslant 2$, are identical to those provided for the corresponding building block of Ref. [2], except for the quantities θ_{11m}. For our displacement-driven building block, they are given as follows.

Solution 1:

$$\theta_{11m} = 1/(\cosh \beta_m + \theta_{1m} \cos \gamma_m).$$

Solution 2:

$$\theta_{11m} = 1/(\cos \beta_m + \theta_{1m} \cos \gamma_m).$$

Solution 3:

$$\theta_{11m} = 1/(\cosh \beta_m + \theta_{1m} \cosh \gamma_m).$$

It will be obvious that the solution for the second building block of Fig. 4 cannot be extracted from that of the first. This was taken care of in Ref. [2] by introducing an intermediate building block. We follow the same procedure here and introduce an intermediate building block identical to the first building block of Fig. 2, except that displacement V is anti-symmetrically distributed about the ξ-axis. Solution for response of our displacement-driven building block differs from that provided in Ref. [2] only in connection with the quantities θ_{11m}. Appropriate expressions for

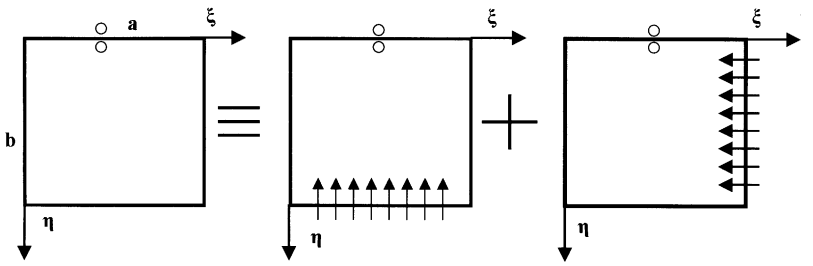

Fig. 4. Building blocks utilized in symmetric–anti-symmetric mode analysis.

these quantities as they relate to the present intermediate building block are as follows:

Solution 1:

$$\theta_{11m} = 1/(\sinh \beta_m + \theta_{1m} \sin \gamma_m).$$

Solution 2:

$$\theta_{11m} = 1/(\sin \beta_m + \theta_{1m} \sin \gamma_m).$$

Solution 3:

$$\theta_{11m} = 1/(\sinh \beta_m + \theta_{1m} \sinh \gamma_m).$$

It will be obvious that a solution for the response of the second building block of Fig. 4 can now be extracted, through a transformation of axes, from that of the intermediate building block described above.

This completes the obtaining of response solutions for all building blocks required in the work undertaken in the present paper.

2.7. Generation of the eigenvalue matrices

A thorough description of development of these matrices for completely free plates was provided in Ref. [2]. Only a brief description of matrix development for the present problem, with emphasis on the way it differs from that described earlier, is therefore provided here.

Well-established procedures are followed. Focusing on the symmetric–symmetric mode analysis of the present problem, we begin by choosing a value for 'N', the number of terms to be utilized in the building block solution expansions. We then turn our attention to the solution of interest, i.e., that composed of the combined solution resulting when the two building block solutions are superimposed, one-upon-the-other. This new solution satisfies all prescribed boundary conditions along the axes, as well as the required condition of zero shear stress along the outer edges. The additional condition to be satisfied by the combined solution along the edge, $\eta = 1$, is now expressed as (Eq. (4)

$$\sigma_y^*(\xi, \eta)|_{\eta=1} + K_1^* V(\xi, \eta)|_{\eta=1} = 0. \tag{28}$$

Each building block will contribute to the left-hand side of the above equation. We choose to expand the contributions of each building block in a trigonometric series and require that each net coefficient in this boundary series should vanish (the superposition method). It is appropriate here to use the trigonometric series of Eq. (16) as the contributions of the first building block will already be available in terms of this series. Contributions of the second building block will need to be expanded in this boundary series using standard techniques. Setting each net coefficient in the boundary series equal to zero gives rise to a set of N homogeneous algebraic equations relating the $2N$ driving coefficients, E_m and E_n. A second set of homogeneous algebraic equations is obtained by enforcing the appropriate boundary condition along the edge, $\xi = 1$. We thus have a set of $2N$ equations relating the $2N$ unknown driving coefficients. The coefficient matrix of this set of equations constitutes our eigenvalue matrix.

A schematic representation of the matrix is shown in Fig. 5. Eigenvalues are obtained by searching for those values of λ^2, the dimensionless frequency, which causes the determinant of this

eigenvalue matrix to vanish. By setting one of the non-zero driving coefficients equal to unity and solving the resulting set of non-homogeneous equations, the remaining coefficients are evaluated and mode shapes of the in-plane displacements are obtained.

An identical procedure is followed to solve for the eigenvalues and mode shapes of the other two mode families. It is to be noted that with the stiffness coefficients K_1^* and K_2^* equal to zero, the above computation will generate eigenvalues of the completely free plate. It is also worth noting that only the diagonal terms of the eigenvalue matrix described will depend on these elastic stiffness coefficients. This is because the second building block has zero displacement normal to the edge, $\eta = 1$, while the first has zero displacement normal to the edge, $\xi = 1$.

It will be obvious that as the elastic stiffness coefficients approach infinity the plate vibration modes will approach certain limits, i.e., limits where motion normal to the plate outer edges must equal zero. We examine these limiting cases next.

2.8. *Analysis of plate vibration limiting simple support cases*

In analogy with plate lateral vibration problems, there are certain sets of boundary conditions for which exact solutions can be obtained. One such family of modes was discussed in Ref. [1] and elaborated upon in Ref. [3]. In this earlier mode family, displacement parallel to the plate outer edges, as well as stress normal to these edges, was not allowed. Exact solutions for these problems were obtained by means of a one-term Levy type solution in Ref. [3].

We now look at a companion set of simply supported plate problems where shear stress along the outer edges, as well as displacement normal to these edges, is not allowed. We will continue to focus attention on quarter-plate segments.

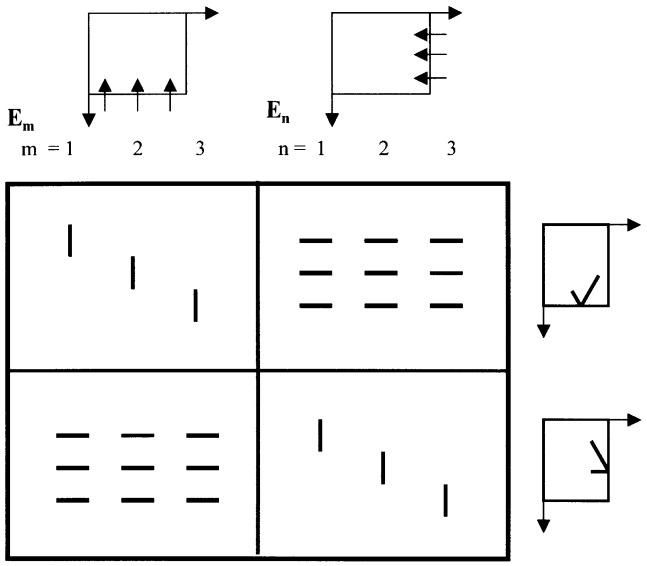

Fig. 5. Schematic representation of eigenvalue matrix based on three-term building block solutions.

2.8.1. Fully symmetric mode vibration

The quarter-plate of interest differs from that of Fig. 2 only in the boundary conditions to be enforced. In what is to follow we express the required solution in a manner identical to that provided for the first building block of the general problem of symmetric–symmetric mode vibration analysis described earlier. All of the symbols, with the exception of θ_{11m}, are unchanged. This time, however, we will focus on the response related to each term, m, of the series, individually. Also, we will ignore Solution 3, described earlier, as only trigonometric functions can appear in the simple support mode shapes under study.

For any term, m, we may write

$$V(\xi,\eta) = V_m(\eta)\sin \text{emp}\,\xi \tag{29}$$

and

$$U(\xi,\eta) = U_m(\eta)\cos \text{emp}\,\xi, \tag{30}$$

where $\text{emp} = (2m-1)\pi/2$.

Enforcing the condition of symmetry about the ξ-axis, and zero shear stress along the edge, $\eta = 1$, we obtain

Solution 1:

$$V_m(\eta) = A_m[\cosh\,\beta_m\eta + \theta_{1m}\cos\,\gamma_m\eta] \tag{31}$$

and

$$U_m(\eta) = A_m[\alpha_{2m}\sinh\,\beta_m\eta + \theta_{1m}\alpha_{4m}\sin\,\gamma_m\eta]. \tag{32}$$

Solution 2:

$$V_m(\eta) = A_m[\cos\,\beta_m\eta + \theta_{1m}\cos\,\gamma_m\eta] \tag{33}$$

and

$$U_m(\eta) = A_m[\alpha_{2m}\sin\,\beta_m\eta + \theta_{1m}\alpha_{4m}\sin\,\gamma_m\eta]. \tag{34}$$

Note that required conditions of zero shear stress and zero normal displacement along the edge, $\xi = 1$, are satisfied.

It is now necessary to evaluate the constant A_m. It is advantageous to consider the edge, $\eta = 1$, to be driven by a harmonic normal stress of distributed amplitude, $E_m \sin \text{emp}\,\xi$.

Substituting for the expression σ_y^*, from the above equations, and setting this quantity equal to the applied stress at the driven edge, we obtain the following.

Solution 1:

$$V_m(\eta) = E_m\theta_{11m}[\cosh\,\beta_m\eta + \theta_{1m}\cos\,\gamma_m\eta] \tag{35}$$

and

$$U_m(\eta) = E_m\theta_{11m}[\alpha_{2m}\sinh\,\beta_m + \theta_{1m}\alpha_{4m}\sin\,\gamma_m\eta], \tag{36}$$

where

$$\theta_{11m} = 1/\{[\beta_m/\phi - \nu\,\text{emp}\,\alpha_{2m}]\sinh\,\beta_m - \theta_{1m}[\gamma_m/\phi + \nu\,\text{emp}\,\alpha_{4m}]\sin\,\gamma_m\}.$$

Solution 2:

$$V_m(\eta) = E_m\theta_{11m}[\cos\ \beta_m\eta + \theta_{1m}\ \cos\ \gamma_m\eta] \tag{37}$$

and

$$U_m(\eta) = E_m\theta_{11m}[\alpha_{2m}\ \sin\ \beta_m\eta + \theta_{1m}\alpha_{4m}\ \sin\ \gamma_m\eta], \tag{38}$$

where

$$\theta_{11m} = -1/\{[\beta_m/\phi + \nu\,\mathrm{emp}\,\alpha_{2m}]\ \sin\ \beta_m + \theta_{1m}[\gamma_m/\phi + \nu\,\mathrm{emp}\,\alpha_{4m}]\ \sin\ \gamma_m\}.$$

Eigenvalues for the family of simple support modes under consideration are obtained as follows.

First, choose a value for the quantity 'm' of interest. Then enforce the condition of zero displacement normal to the edge, $\eta = 1$. This requires searching for the value of the parameter λ^2, which causes the quantity to the right of the coefficient E_m of Eqs. (35) or (37) to vanish, thus permitting a non-trivial solution for plate displacement. These values of λ^2 are the eigenvalues. Mode displacements are given by Eqs. (35) and (36), or (37) and (38), as appropriate.

It is found that when Solution 1 is applicable the coefficient of the hyperbolic term vanishes and this term can be neglected. There are, in theory, an infinite number of eigenvalues associated with any value of the subscript 'm', but only the first four or five will be of interest to us.

2.8.2. *Anti-symmetric–anti-symmetric mode vibration*

The procedure to be followed here is essentially the same as that described above for the symmetric–symmetric modes. For any value of 'm', the plate displacements are now expressed as (see Eqs. (22) and (23))

$$V_m(\xi,\eta) = V_m(\eta)\cos\ \mathrm{emp}\,\xi \tag{39}$$

and

$$U_m(\xi,\eta) = U_m(\eta)\sin\ \mathrm{emp}\,\xi, \tag{40}$$

where $\mathrm{emp} = (m-1)\pi$.

Here we encounter a special case when the subscript m equals one. As pointed out in the earlier study of these modes, the quantity $U_m(\eta)$ will equal zero and for $V_m(\eta)$ we have (Eq. (24))

$$V_m(\eta) = A_0\ \sin\ \alpha\eta, \tag{41}$$

where $\alpha^2 = \lambda^2\phi^2/a_{11}, a_{11} = 1.0$, and A_0 is a constant to be determined.

The driving harmonic stresses at the edge, $\eta = 1$, of the plate for this family of modes is obtained from the cosine series of Eq. (25). The first term of this series will be a constant, E_m, where $m = 1$, and it must balance the stress at the plate boundary. This latter stress is obtained by substituting Eq. (41) into the expression for the dimensionless stress σ_y^*. We thus obtain for the constant A_0,

$$A_0 = \frac{E_m\phi}{\alpha\ \cos\ \alpha}, \tag{42}$$

and for the displacement of the driven edge,

$$V(\eta)|_{\eta=1} = E_m \frac{\phi \sin \alpha}{\alpha \cos \alpha}. \tag{43}$$

Setting the displacement equal to zero, it is seen that a non-trivial solution for the quantity E_m is obtained only if the parameter α takes on the discrete values $\pi, 2\pi, \ldots\ldots, n\pi$, etc. Returning to the definition of α, we find that we can write for the eigenvalue associated with any plate, for $m = 1$,

$$\lambda^2 = n\pi/\phi. \tag{44}$$

We thus have available the eigenvalues and mode shapes for this mode family with $m = 1$. No computations are required.

It will be appreciated that two distinct one-dimensional free vibration modes of the type described above are possible. In the second mode of this pair, displacement will be a function of the coordinate, ξ, only. Solutions for eigenvalues and mode shapes of this latter set are easily extracted from the solution described above by simply replacing the plate aspect ratio with its inverse. Eq. (44) would lead, however, to eigenvalues based on edge length 'b'. We can retain our definition, based on edge length 'a', through multiplying the right-hand side of Eq. (44) by the inverse of the aspect ratio. This leads to the following modified expression for the eigenvalues of these latter problems:

$$\lambda^2 = n\pi. \tag{45}$$

We next look at the analysis when $m \geqslant 2$. Following steps completely analogous to those described for symmetric–symmetric mode analysis immediately above, we arrive at expressions for the quantities $V_m(\eta)$ and $U_m(\eta)$ as follows.

Solution 1:

$$V_m(\eta) = E_m \theta_{11m} [\sinh \beta_m \eta + \theta_{1m} \sin \gamma_m \eta] \tag{46}$$

and

$$U_m(\eta) = E_m \theta_{11m} [\alpha_{1m} \cosh \beta_m \eta + \theta_{3m} \cos \gamma_m \eta], \tag{47}$$

with

$$\theta_{11m} = 1 \Big/ \left\{ \left[\frac{\beta_m}{\phi} + v \operatorname{emp} \alpha_{1m} \right] \cosh \beta_m + \theta_{1m} \left[\frac{\gamma_m}{\phi} + v \operatorname{emp} \alpha_{3m} \right] \cos \gamma_m \right\}.$$

Solution 2:

$$V_m(\eta) = E_m \theta_{11m} [\sin \beta_m \eta + \theta_{1m} \sin \gamma_m \eta] \tag{48}$$

and

$$U_m(\eta) = E_m \theta_{11m} [\alpha_{1m} \cos \beta_m \eta + \theta_{1m} \alpha_{3m} \cos \gamma_m \eta], \tag{49}$$

with

$$\theta_{11m} = 1 \Big/ \left\{ \left[\frac{\beta_m}{\phi} + v \operatorname{emp} \alpha_{1m} \right] \cos \beta_m + \theta_{1m} \left[\frac{\gamma_m}{\phi} + v \operatorname{emp} \alpha_{3m} \right] \cos \gamma_m \right\}.$$

Again, eigenvalues are obtained by searching for those values of the parameter λ^2 which cause the quantity to the right of the coefficient E_m in the appropriate expression for $V_m(\eta)$ to vanish.

2.8.3. Symmetric–anti-symmetric mode vibration

Here we focus attention on the first building block of Fig. 4. For any value of 'm', the plate displacements are again expressed as given by Eqs. (39) and (40). Now, with subscript 'm' equal to one, it is shown that

$$V_m(\eta) = A_0 \cos \alpha\eta, \tag{50}$$

while $U_m(\eta)$ equals zero everywhere. The amplitude of the driving stress is expressed as E_m cos emp, and enforcing a balance between the plate normal stress and the driving stress at the boundary we obtain

$$V_m(\eta) = -\frac{E_m\phi}{\alpha \sin \alpha} \cos \alpha. \tag{51}$$

It is seen that for a non-trivial solution for this displacement, with E_m not equal to zero, we require

$$\alpha = (2n-1)\pi/2, \quad n = 1, 2, \ldots, \text{etc.} \tag{52}$$

and for the frequencies we have, after rearrangement,

$$\lambda^2 = \frac{(2n-1)}{\phi}\pi/2. \tag{53}$$

In this mode family, there will be no one-dimensional mode with displacement a function of the coordinate ξ.

We turn next to the situation when $m \geqslant 2$. Again, we follow steps analogous to those described for the symmetric–symmetric mode studies and arrive at the following expressions for the quantities $V_m(\eta)$ and $U_m(\eta)$.

Solution 1:

$$V_m(\eta) = E_m\theta_{11m}[\cosh \beta_m\eta + \theta_{1m} \cos \gamma_m\eta] \tag{54}$$

and

$$U_m(\eta) = E_m\theta_{11m}[\alpha_{2m} \sinh \beta_m\eta + \theta_{1m}\alpha_{4m} \sin \gamma_m\eta], \tag{55}$$

with

$$\theta_{11m} = 1 \Big/ \left\{ \left[\frac{\beta_m}{\phi} + v \operatorname{emp} \alpha_{2m}\right] \sinh \beta_m - \theta_{1m}\left[\frac{\gamma_m}{\phi} - v \operatorname{emp} \alpha_{4m}\right] \sin \gamma_m \right\}.$$

Solution 2:

$$V_m(\eta) = E_m\theta_{11m}[\cos \beta_m\eta + \theta_{1m} \cos \gamma_m\eta] \tag{56}$$

and

$$U_m(\eta) = E_m\theta_{11m}[\alpha_{2m} \sin \beta_m\eta + \theta_{1m}\alpha_{4m} \sin \gamma_m\eta], \tag{57}$$

with

$$\theta_{11m} = 1 \Big/ \left\{ \left[v \operatorname{emp} \alpha_{2m} - \frac{\beta_m}{\phi}\right] \sin \beta_m + \theta_{1m}\left[v \operatorname{emp} \alpha_{4m} - \frac{\gamma_m}{\phi}\right] \sin \gamma_m \right\}.$$

Again, eigenvalues are those values of the parameter λ^2 which cause the quantities to the right of the coefficient E_m in Eqs. (54) or (56), as appropriate, to vanish.

3. Presentation of computed results

There are well-defined upper and lower frequency limits for free vibration of the elastically supported rectangular plates considered here. We begin with a tabulation of the lower limits for a selected range of plate aspect ratios.

3.1. Completely free plate vibration eigenvalues

A limited tabulation of accurate eigenvalues for the completely free plate was presented in Ref. [2], where excellent agreement with those computed earlier by Bardel et al. [1] was obtained. Here, using the displacement-driven building blocks described, a more comprehensive set of eigenvalues is provided. Computed results for each of the three mode families are tabulated separately in Tables 1–4 with plate aspect ratios of 1.0, 1.25, 1.50, and 2.0. In the case of symmetric–anti-symmetric modes, results are also presented for the inverse of these aspect ratios. The objective has been to provide results with four significant digit accuracy. Based on the experience described in Ref. [2], it has been chosen to utilize 15 terms in all building block series solutions in order to assure the required accuracy.

It will be seen that, except for a very few cases, the lower limits for free vibration of the elastically supported plate will be those of the completely free plate. Exceptional cases will be

Table 1
Computed eigenvalues, λ^2, for symmetric–symmetric mode vibration of the completely free plate

Mode	φ			
	1.0	1.25	1.5	2.0
(1)	1.160	1.043	0.9604	0.8170
(2)	2.153	1.825	1.531	1.182
(3)	2.629	2.303	2.083	1.714
(4)	2.643	2.506	2.364	1.987

Table 2
Computed eigenvalues, λ^2, for anti-symmetric–anti-symmetric mode vibration of the completely free plate

Mode	φ			
	1.0	1.25	1.5	2.0
(1)	1.314	1.136	0.9716	0.7402
(2)	1.494	1.362	1.351	1.308
(3)	1.726	1.612	1.577	1.501
(4)	2.523	2.101	1.859	1.585

Table 3
Computed eigenvalues, λ^2, for symmetric–anti-symmetric mode vibration of the completely free plate ($\varphi \geqslant 1$)

Mode	φ			
	1.0	1.25	1.5	2.0
(1)	1.236	1.292	1.324	1.314
(2)	1.862	1.661	1.510	1.342
(3)	2.485	2.219	2.065	1.687
(4)	3.050	2.500	2.124	1.863

Table 4
Computed eigenvalues, λ^2, for symmetric–anti-symmetric mode vibration of the completely free plate ($\varphi^{|} \geqslant 1$)

Mode	$\varphi^{|}$			
	1.0	1.25	1.5	2.0
(1)	1.236	1.166	1.099	0.9774
(2)	1.862	2.049	2.190	2.392
(3)	2.485	2.841	3.072	3.225
(4)	3.050	3.460	3.808	4.465

Table 5
Simply supported plate eigenvalues, λ^2: symmetric–symmetric modes

	$\varphi = 1$				$\varphi = 1.25$			
n:	(1)	(2)	(3)	(4)	(1)	(2)	(3)	(4)
m:								
(1)	1.314	2.221	2.939	4.738	1.190	2.012	2.416	3.832
(2)	2.939	3.943	4.967	5.419	2.885	3.570	4.647	4.877
(3)	4.738	5.419	6.571	7.994	4.706	5.154	5.950	6.977
(4)	6.571	7.007	7.994	9.200	6.547	6.876	7.492	8.330

those where, as the elastic support coefficients approach zero, the plate is able to approach limits of rigid body rotation or translation. Such cases will be drawn to the attention of the reader.

3.2. Computed eigenvalues for the simply supported mode family

As pointed out earlier, the simply supported mode family considered here involves mode shapes where shear stresses along the plate edges, as well as displacements normal to these edges, are everywhere zero. Eigenvalues for these modes constitute upper limits for the elastically supported plate. Exact solutions for these eigenvalues are now available and they are tabulated in Tables 5–12. The letter 'm' indicates the number of half waves running along the edge, $\eta = 1$, while the letter 'n' indicates the associated modes in ascending order.

3.3. Computed eigenvalues for elastically supported plates

Computed eigenvalues for elastically supported plates of various aspect ratios and with various elastic stiffness coefficients are presented in Tables 13–20. It is to be noted that for all results presented in these tables the two dimensionless stiffness coefficients, K_1^* and K_2^*, are equal. In each

Table 6
Simply supported plate eigenvalues, λ^2: symmetric–symmetric modes

	$\varphi = 1.5$				$\varphi = 2.0$			
n:	(1)	(2)	(3)	(4)	(1)	(2)	(3)	(4)
m:								
(1)	1.169	1.888	2.078	3.234	1.039	1.675	1.756	2.502
(2)	2.856	3.351	4.168	4.827	2.826	3.117	3.629	4.284
(3)	4.688	5.004	5.584	6.356	4.670	4.851	5.195	5.672
(4)	6.535	6.765	7.205	7.818	6.522	6.653	6.907	7.272

Table 7
Simply supported plate eigenvalues, λ^2: anti-symmetric–anti-symmetric modes

	$\varphi = 1$				$\varphi = 1.25$			
n:	(1)	(2)	(3)	(4)	(1)	(2)	(3)	(4)
m:								
(1)[a]	3.142	6.283	9.425	12.57	2.513	5.027	7.540	10.05
(2)[b]	3.142	6.283	9.425	12.57	3.142	6.283	9.425	12.57
(3)	2.629	4.156	4.443	5.877	2.380	3.507	4.023	4.832
(4)	4.156	5.257	6.701	7.025	4.004	4.760	5.806	6.767

[a] $u = 0$.
[b] $v = 0$.

Table 8
Simply supported plate eigenvalues, λ^2: anti-symmetric–anti-symmetric modes

	$\varphi = 1.5$				$\varphi = 2.0$			
n:	(1)	(2)	(3)	(4)	(1)	(2)	(3)	(4)
m:								
(1)[a]	2.094	4.189	6.283	8.378	1.501	3.142	4.712	6.283
(2)[b]	3.142	6.283	9.425	12.57	3.142	6.283	9.425	12.57
(3)	2.234	3.098	3.776	4.156	2.078	2.628	3.351	3.512
(4)	3.918	4.468	5.257	6.195	3.832	4.156	4.647	5.257

[a] $u = 0$.
[b] $v = 0$.

Table 9
Simply supported plate eigenvalues, λ^2: symmetric–anti-symmetric modes

	$\varphi = 1.0$				$\varphi = 1.25$			
n:	(1)	(2)	(3)	(4)	(1)	(2)	(3)	(4)
m:								
(1)[a]	1.571	4.712	7.854	11.00	1.257	3.770	6.283	8.797
(2)	2.078	3.351	3.512	5.004	2.002	2.903	3.384	4.156
(3)	3.832	4.647	5.950	6.477	3.791	4.335	5.257	6.395
(4)	5.653	6.234	7.258	8.568	5.625	6.005	6.701	7.627

[a] $u = 0$.

Table 10
Simply supported plate eigenvalues, λ^2: symmetric–anti-symmetric modes

	$\varphi = 1.5$				$\varphi = 2.0$			
n:	(1)	(2)	(3)	(4)	(1)	(2)	(3)	(4)
m:								
(1)[a]	1.047	3.142	5.236	7.330	0.7854	2.356	3.927	5.498
(2)	1.959	2.628	3.312	3.613	1.916	2.323	2.975	3.238
(3)	3.769	4.156	4.839	5.712	3.970	4.384	4.939	5.595
(4)	5.877	6.379	7.064	7.885	5.747	6.455	6.970	7.564

[a] $u = 0$.

Table 11
Simply supported plate eigenvalues, λ^2: symmetric–anti-symmetric modes

	$\varphi^{\mathrm{l}} = 1.0$				$\varphi^{\mathrm{l}} = 1.25$			
n:	(1)	(2)	(3)	(4)	(1)	(2)	(3)	(4)
m:								
(1)[a]	1.571	4.712	7.854	11.00	1.964	5.891	9.818	1.375
(2)	2.078	3.351	3.512	5.004	2.192	3.705	3.950	6.098
(3)	3.832	4.647	5.950	6.477	3.895	5.095	6.583	6.896
(4)	5.653	6.234	7.258	8.568	5.696	6.575	8.051	9.627

[a] $u = 0$.

table the first column gives the lower limit eigenvalues, which are obtained from the completely free plate eigenvalue tabulations, or are, in fact, equal to zero if rigid body motion of the plate is possible. Upper limit eigenvalues ($K_1^* = \infty$) are obtained from appropriate simply supported plate eigenvalue tabulations.

Table 12
Simply supported plate eigenvalues, λ^2: symmetric–anti-symmetric modes

	$\varphi^{\mid} = 1.5$				$\varphi^{\mid} = 2.0$			
n:	(1)	(2)	(3)	(4)	(1)	(2)	(3)	(4)
m:								
(1)[a]	1.356	7.069	11.78	16.49	3.142	9.925	15.71	21.99
(2)	2.323	3.927	4.576	7.735	2.628	4.443	5.877	9.477
(3)	3.970	5.595	6.710	7.899	4.156	6.701	7.025	10.01
(4)	5.747	6.970	8.926	9.715	5.877	7.885	9.935	10.84

[a] $u = 0$.

Table 13
Eigenvalues vs. stiffness coefficients: symmetric–symmetric modes

	$\varphi = 1$						$\varphi = 1.25$					
K_1^*:	0.0	0.25	0.5	0.75	1.0	∞	0.0	0.25	0.5	0.75	1.0	∞
Mode:												
(1)	0.0	0.4722	0.6331	0.7380	0.8140	1.314	0.0	0.4511	0.6020	0.6989	0.7681	1.190
(2)	1.160	1.271	1.362	1.438	1.502	2.221	1.043	1.153	1.241	1.313	1.373	2.012
(3)	2.153	2.257	2.343	2.414	2.473	2.939	1.825	1.908	1.974	2.027	2.069	2.416

Table 14
Eigenvalues vs. stiffness coefficients: symmetric–symmetric modes

	$\varphi = 1.5$						$\varphi = 2.0$					
K_1^*:	0.0	0.25	0.5	0.75	1.0	∞	0.0	0.25	0.5	0.75	1.0	∞
Mode:												
(1)	0.0	0.4440	0.5910	0.6842	0.7499	1.117	0.0	0.4446	0.5909	0.6823	0.7452	1.039
(2)	0.9604	1.071	1.157	1.226	1.284	1.888	0.8170	0.9394	1.029	1.099	1.155	1.675
(3)	1.531	1.603	1.660	1.706	1.744	2.078	1.182	1.241	1.289	1.329	1.364	1.756

Table 15
Eigenvalues vs. stiffness coefficients: anti-symmetric–anti-symmetric modes

	$\varphi = 1$						$\varphi = 1.25$					
K_1^*:	0.0	0.25	0.5	0.75	1.0	∞	0.0	0.25	0.5	0.75	1.0	∞
Mode:												
(1)	1.314	1.481	1.612	1.717	1.804	2.629	1.136	1.292	1.413	1.523	1.605	2.380
(2)	1.494	1.648	1.776	1.884	1.978	3.142	1.362	1.512	1.611	1.693	1.763	2.380
(3)	1.726	1.841	1.940	2.026	2.100	3.142	1.612	1.716	1.808	1.889	1.961	2.513

Table 16
Eigenvalues vs. stiffness coefficients: anti-symmetric–anti-symmetric modes

	$\varphi = 1.5$						$\varphi = 2.0$					
K_1^*:	0.0	0.25	0.5	0.75	1.0	∞	0.0	0.25	0.5	0.75	1.0	∞
Mode:												
(1)	0.9716	1.121	1.243	1.334	1.408	2.094	0.7402	0.8801	0.9876	1.063	1.122	1.571
(2)	1.351	1.452	1.535	1.603	1.661	2.094	1.308	1.375	1.422	1.457	1.483	1.571
(3)	1.577	1.670	1.752	1.827	1.894	2.234	1.501	1.568	1.612	1.642	1.667	2.078

Table 17
Eigenvalues vs. stiffness coefficients: symmetric–anti-symmetric modes

	$\varphi = 1.0$						$\varphi = 1.25$					
K_1^*:	0.0	0.25	0.5	0.75	1.0	∞	0.0	0.25	0.5	0.75	1.0	∞
Mode:												
(1)	0.0	0.4785	0.6498	0.7663	0.8540	1.571	0.0	0.4234	0.5697	0.6664	0.7376	1.257
(2)	1.236	1.366	1.465	1.541	1.602	2.078	1.292	1.401	1.487	1.554	1.608	2.002
(3)	1.862	1.988	2.097	2.192	2.276	3.351	1.661	1.777	1.876	1.963	2.038	2.903

Table 18
Eigenvalues vs. stiffness coefficients: symmetric–anti-symmetric modes

	$\varphi = 1.5$						$\varphi = 2.0$					
K_1^*:	0.0	0.25	0.5	0.75	1.0	∞	0.0	0.25	0.5	0.75	1.0	∞
Mode:												
(1)	0.0	0.3825	0.5100	0.5922	0.6514	1.047	0.0	0.3244	0.4255	0.4875	0.5305	0.7854
(2)	1.324	1.423	1.500	1.562	1.612	1.959	1.314	1.403	1.478	1.543	1.598	1.916
(3)	1.510	1.615	1.704	1.781	1.848	2.628	1.342	1.433	1.505	1.563	1.611	2.323

Table 19
Eigenvalues vs. stiffness coefficients: symmetric–anti-symmetric modes

	$\phi^{\mid} = 1.0$						$\phi^{\mid} = 1.25$					
K_1^*:	0.0	0.25	0.5	0.75	1.0	∞	0.0	0.25	0.5	0.75	1.0	∞
Mode:												
(1)	0.0	0.4785	0.6498	0.7663	0.8540	1.571	0.0	0.5397	0.7385	0.8769	0.9832	1.964
(2)	1.236	1.366	1.465	1.541	1.602	2.078	1.166	1.324	1.440	1.530	1.602	2.192
(3)	1.862	1.988	2.097	2.192	2.276	3.351	2.049	2.185	2.304	2.407	2.497	3.705

Table 20
Eigenvalues vs. stiffness coefficients: symmetric–anti-symmetric modes

	$\varphi^{\mid} = 1.5$						$\varphi^{\mid} = 2.0$					
K_1^*:	0.0	0.25	0.5	0.75	1.0	∞	0.0	0.25	0.5	0.75	1.0	∞
Mode:												
(1)	0.0	0.5946	0.8180	0.9760	1.099	2.323	0.0	0.6917	0.9580	1.150	1.303	2.928
(2)	1.099	1.287	1.423	1.526	1.609	2.323	0.9774	1.231	1.406	1.539	1.644	3.142
(3)	2.190	2.342	2.472	2.584	2.681	3.927	2.392	2.583	2.739	2.868	2.978	4.156

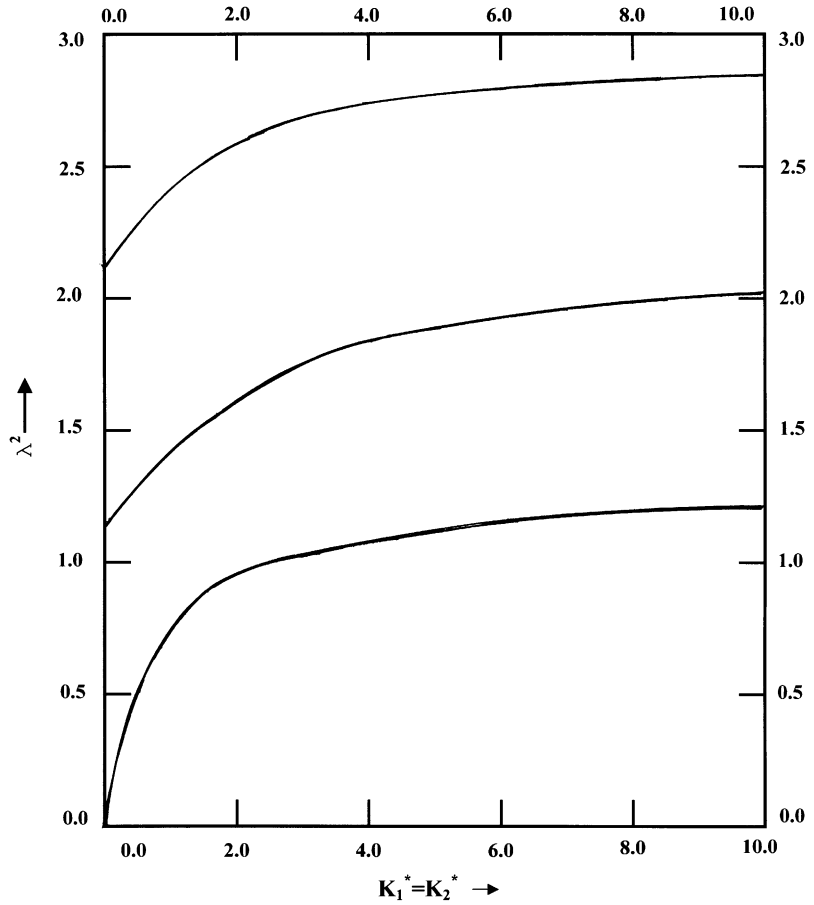

Fig. 6. Graphical representation of first three symmetric–symmetric mode eigenvalues as a function of elastic edge support coefficient for square plate ($K_1^* = K_2^*$).

4. Discussion of results

In Fig. 6, eigenvalues for the first three fully symmetric modes of the square plate are plotted as a function of the dimensionless elastic edge coefficients. As the stiffness coefficients approach zero the plate approaches a condition of rigid body in-plane oscillatory rotation about the quarter plate upper left corner. This is, of course, the center point of the full plate.

In Fig. 7 the computed mode shape is shown for the above quarter plate with dimensionless stiffness coefficients equal to 0.05. It will be noted that at this low value of elastic edge support stiffness the quarter plate almost retains its rectangular configuration but is able to oscillate about the origin of its axes. It should also be noted that symmetric mode conditions are satisfied along the same axes.

We next turn to the upper limit for this mode as the stiffness coefficients approach infinity. The exact eigenvalue related to this limit is, of course, available from Table 5 and is equal to 1.314. Extending the first mode plot of Fig. 7 to higher stiffness values it is found that, in fact, one approaches arbitrarily close to the above eigenvalue. With a stiffness coefficient of 100, the associated eigenvalue is found to equal 1.305.

The computed mode shape related to the exact eigenvalue (based on the simply supported plate analysis) is presented in Fig. 8. It will be noted that the condition of zero displacement normal to

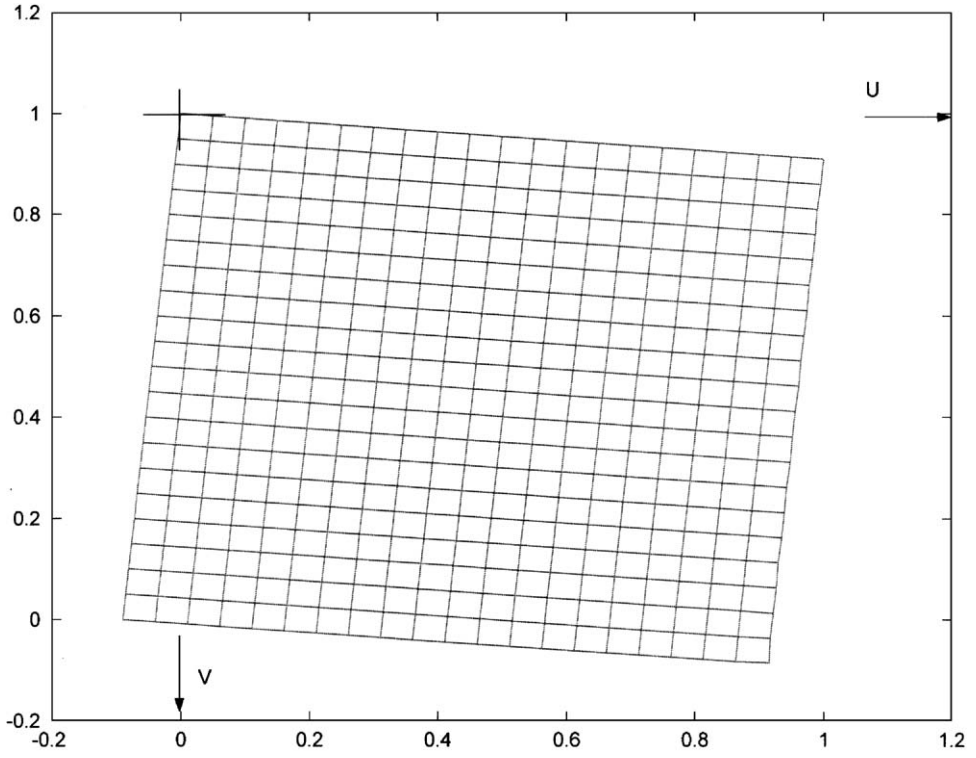

Fig. 7. Computed mode shape for first symmetric–symmetric mode vibration of elastically supported square plate ($K_1^* = K_2^* = 0.05$).

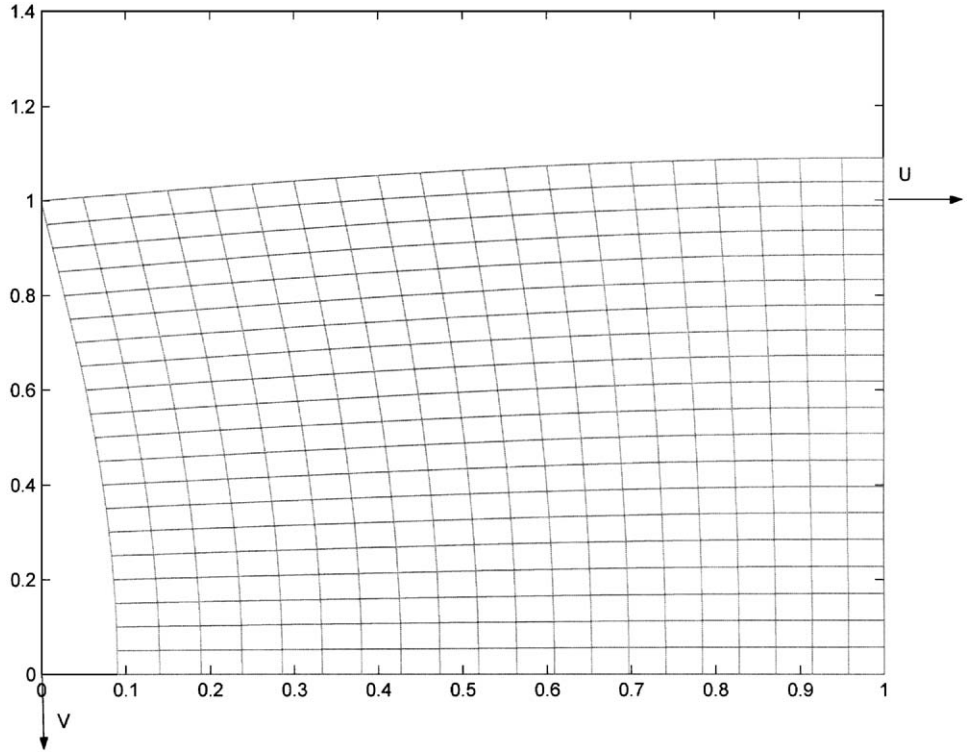

Fig. 8. Computed mode shape for first symmetric–symmetric mode vibration of the simply supported square plate.

the plate outer edges is fulfilled exactly. The condition of zero shear stress along these edges is, of course, also satisfied.

In Fig. 9 the corresponding mode shape obtained from the elastically supported plate analysis, based on a dimensionless stiffness coefficient of 100, is also presented. It will be observed on comparing the two mode shapes above that they are almost identical.

Extended verification curves of the type shown in Fig. 6 have been plotted in connection with all of the elastically supported plate free vibration computed data presented in Tables 13–20. In each case the approach of the curves to the correct upper limit was verified. This adds a high degree of confidence to the analytical procedures employed.

In Tables 17–20, which relate to symmetric–anti-symmetric mode vibration, it will be observed that the first mode eigenvalue with K_1^* equal to zero is also zero. This limit of zero for the eigenvalue corresponds to plate rigid body translation parallel to the η-axis.

5. Discussion and conclusions

Research of a limited scope related to in-plane free vibration of plates with elastic support along one edge is reported by Gutierrez and Laura [6]. What was described as 'an approximate solution' obtained by the Ritz approach was utilized to generate a very limited amount of computed data.

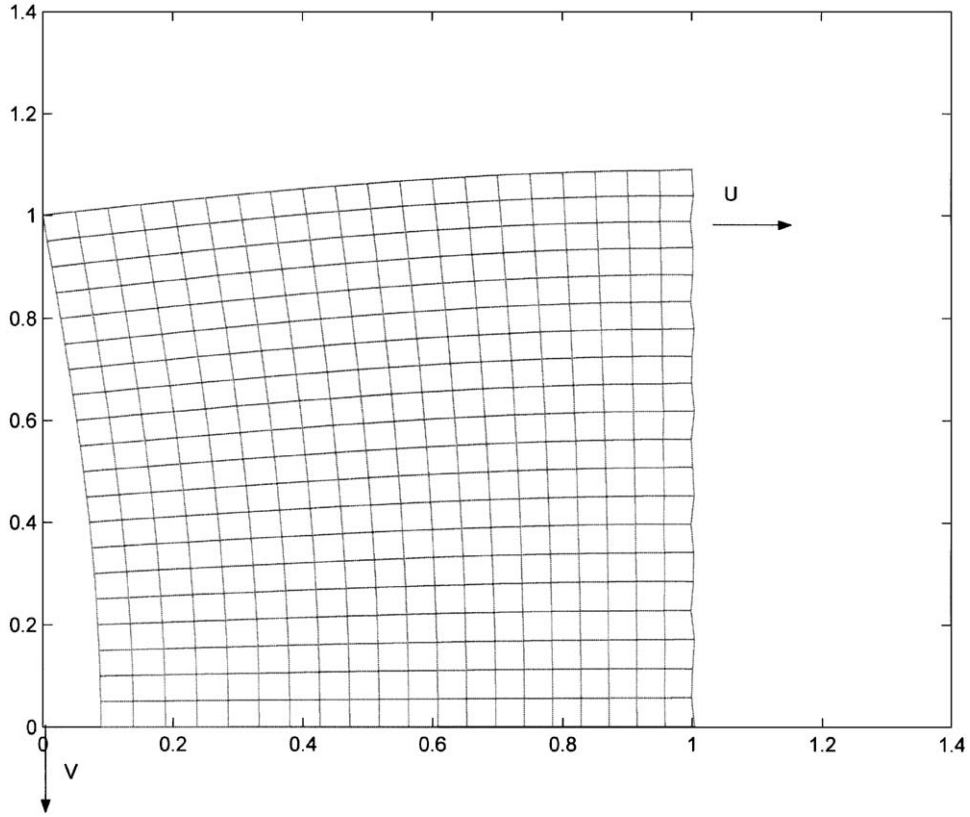

Fig. 9. Computed mode shape for first symmetric–symmetric mode vibration of elastically supported square plate ($K_1^* = K_2^* = 100$).

In the present paper, the primary objective has been to obtain an accurate analytical type solution for the free in-plane vibration of rectangular plates with symmetrically distributed uniform elastic supports acting normal to the edges. Toward this end, it was decided to extend the superposition method as described in Ref. [2] in order to accomplish the task. Building blocks utilized in the earlier analysis were slightly modified to the edge-displacement driven type in order to avoid the possibility of uncovering rejection mode eigenvalues as discussed earlier. A substantially increased tabulation of accurate eigenvalues for the completely free plate are now available in Tables 1–4. These eigenvalues also, of course, provide lower limits for those of the elastically supported plates.

It was recognized that upper limits for the eigenvalues of elastically supported plates were, in fact, those of a family of 'simply supported' plates for which exact solutions were achievable. Exact single-term Levy type solutions for this latter family of plates were obtained and results tabulated. Finally, a rather extensive array of computed eigenvalues for elastically supported plates of various aspect ratios and elastic edge stiffness coefficients was provided. It has been verified that correct limiting cases have been approached as elastic support coefficients approach

their natural limits. It is anticipated that all data tabulated here will serve a valuable role in providing accurate results against which the findings of other researchers can be compared.

It will be appreciated by the reader that only a limited range of eigenvalues can be tabulated for these elastically supported plates. One could compute eigenvalues for plates with two opposite edges elastically supported and the other two free by simply setting one of the elastic coefficients, K_1^*, or K_2^* equal to zero. It will be apparent that the same basic analytical procedure described here could be utilized to study the free vibration of plates where the elastic support is not symmetrically distributed about the plate central axes. This could be accomplished by utilizing a single set of three or four building blocks, as required, so that prescribed boundary conditions could be satisfied along each edge. While in the present study all edges are considered to be free of shear, this condition can be altered. In fact, it is evident that, with the correct choice of building blocks, the present method can be exploited to handle plates with any combination of classical or elastically supported edge conditions.

References

[1] N.S. Bardell, R.S. Langley, J.M. Dunsdon, On the free in-plane vibration of isotropic rectangular plates, *Journal of Sound and Vibration* 191 (3) (1996) 459–467.

[2] D.J. Gorman, Free in-plane vibration analysis of rectangular plates by the method of superposition, *Journal of Sound and Vibration* 272 (2004) 831–851.

[3] D.J. Gorman, Accurate analytical type solutions for the free in-plane vibration of clamped and simply supported rectangular plates, *Journal of Sound and Vibration* 276 (2004) 311–333.

[4] G. Wang, N.M. Werely, Free in-plane vibration of rectangular plates, *AIAA Journal* 40 (5) (2002) 953–959.

[5] D.J. Gorman, *Vibration Analysis of Plates by the Method of Superposition*, World Scientific, Singapore, 1999.

[6] R.H. Gutierrez, P.A.A. Laura, In-plane vibration of thin elastic rectangular plates elastically restrained against translation along the edges, *Journal of Sound and Vibration* 132 (3) (1998) 512–515.